TPF-5(433) Behavior of Reinforced and Unreinforced Lightweight Cellular Concrete (LCC) For Retaining Walls

Interim Report on Test of MSE Wall with Lightweight Cellular Concrete Backfill

Prepared by

Prof. Kyle M. Rollins

Civil & Environmental Engineering Dept.
Brigham Young University
430 EB, Provo, UT 84602

Prepared for

David Stevens, Project Manager

Research & Innovation Division
Utah Department of Transportation
4501 S. 2700 W.
Salt Lake City, UT 84114

August 8, 2020

Background

This test is the first test conducted MSE wall test conducted with reinforced lightweight cellular concrete (LCC) backfill under Transportation Pooled Fund Study TPF-5(433). Previous tests were performed using unreinforced LCC backfill behind a reinforced concrete cantilever (RCC) wall. Comparisons to the unreinforced backfill tests are discussed subsequently.

Test Set-up

Schematic plan and profile drawings for the unreinforced LCC test are shown in Fig. 1. The test box is 10 ft tall x 12 ft long x 10 ft wide. The MSE wall panels were nominally 5 ft tall by 10 ft wide and 0.5 ft thick. Reinforcements consisted of ribbed-strip reinforcements that were 60 mm wide and 10 mm thick, provided by Reinforced Earth Company (RECo). The cellular concrete had a unit weight of 27 lbs/ft^3 and an unconfined compressive strength (UCS) of about 100 psi at the time of the load test. The cellular concrete was placed in 2.5-foot thick lifts to a height of 10 feet behind the MSE wall panels over a four-day period (one pour per day). The three steel braced walls (show in red) were stiff enough to constrain lateral movements to less than 0.15 inch at the maximum expected surcharge load of about 64 psi (7200 psf) based on SAP2000 analyses of the steel frame. The test box was designed so that we could apply load independently to six stiff concrete beams (2 ft wide by 10 ft long) using independently activated hydraulic jacks with load cells.

Six Geokon pressure cells were placed at approximately 1.5 ft vertical intervals on the back face of the MSE wall panels to monitor interface pressure on the wall during the backfill placement, curing, and surcharge loading. In addition, two hybrid pressure sensors, developed by Prof. Mark Talesnick (Technion, Haifa, Israel) were installed at depths of 2.5 ft. from the top and bottom of the cantilever wall. Two of these pressure sensors were located approximately 1.5 foot inside the LCC block, while two were located at the LCC-wall interface. Finally, 8 thin-film pressure cells developed by Sensor Products were placed at the center of the four LCC lifts at the LCC-MSE wall interface.

Deformation of the retaining wall, the LCC backfill and the test box was monitored using a series of string potentiometers from fill placement to failure that were connected to a data acquisition system. A digital image correlation (DIC) system was also used to monitor the deflection of the retaining wall face to create a color contour map of wall displacements. Thin electrical cables were installed at eight depths within the LCC backfill and monitored with a time-domain reflectometer (TDR) to identify potential failure plane development during surcharge loading. Finally, at the conclusion of the test, the sides of the box and the surcharge panels were removed to identify shear plane and crack patterns in the LCC.

Loading Procedure

Photographs of the test box just prior to testing the RC retaining wall are provided in Fig. 2. For each test, we applied the surcharge load incrementally at 25,000 lbs to 50,000 lbs load increments or 2.75 to 5.5 psi pressure increments. For the test on the MSE retaining wall, load

was applied to the first three surcharge blocks (6 ft) adjacent to the retaining wall as illustrated schematically in Fig. 3(a). For the test against the free face, with no retaining wall, load was applied to the first two surcharge blocks (6 ft) adjacent to the free face as illustrated schematically in Fig. 3(b).The load was quite uniformly distributed over the three blocks in each case, but settlement under the load could be different. Displacement of each block was monitored with three string potentiometers attached to an independent reference frame.

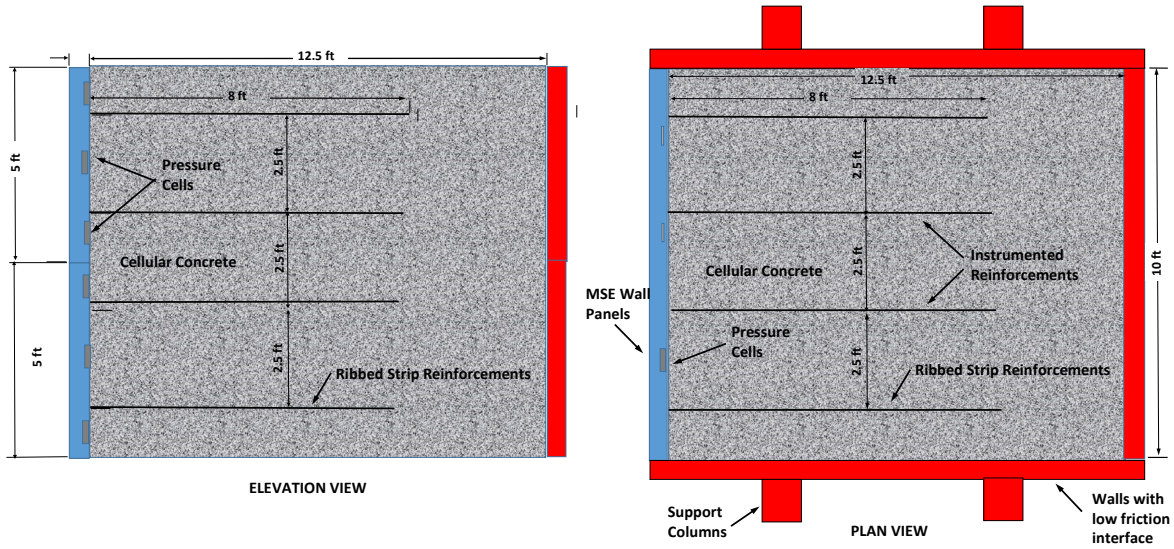

Fig. 1. Schematic plan and profile drawings of the test with unreinforced LCC behind reinforced concrete cantilever retaining wall.

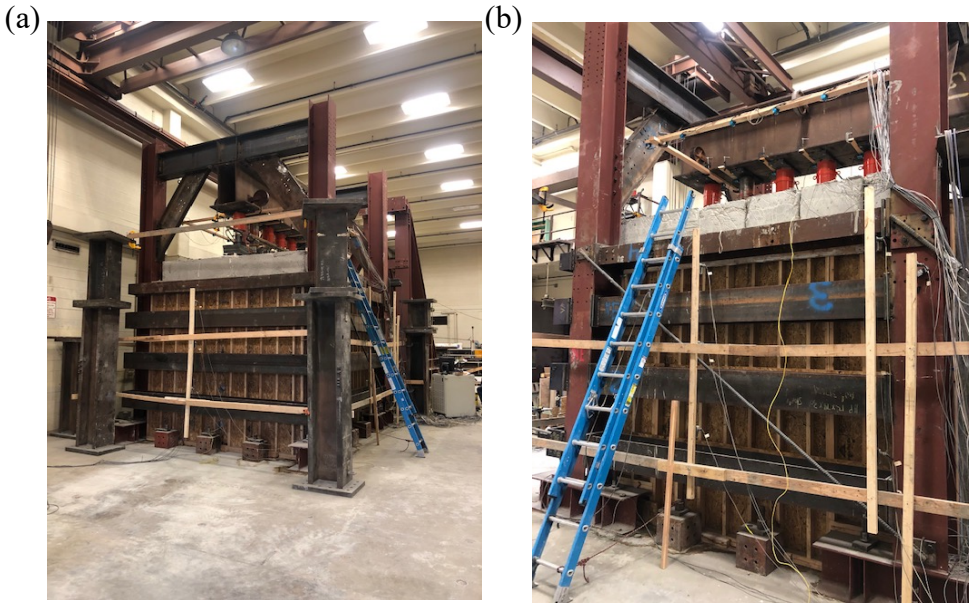

Fig. 2 Photographs showing: (a) the test box from the short side opposite from the retaining wall and (b) the test box from the long side with the concrete surcharge blocks and hydraulic jacks reacting against a longitudinal beam consisting of two deep beams.

(a)

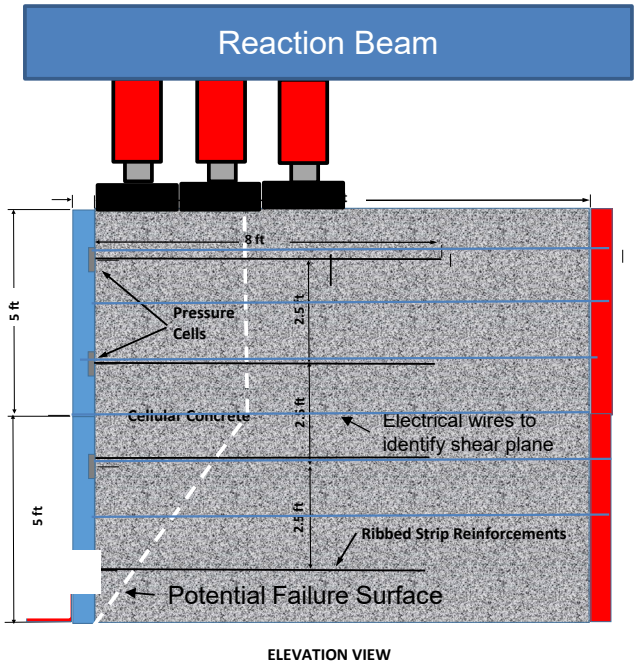

(b)

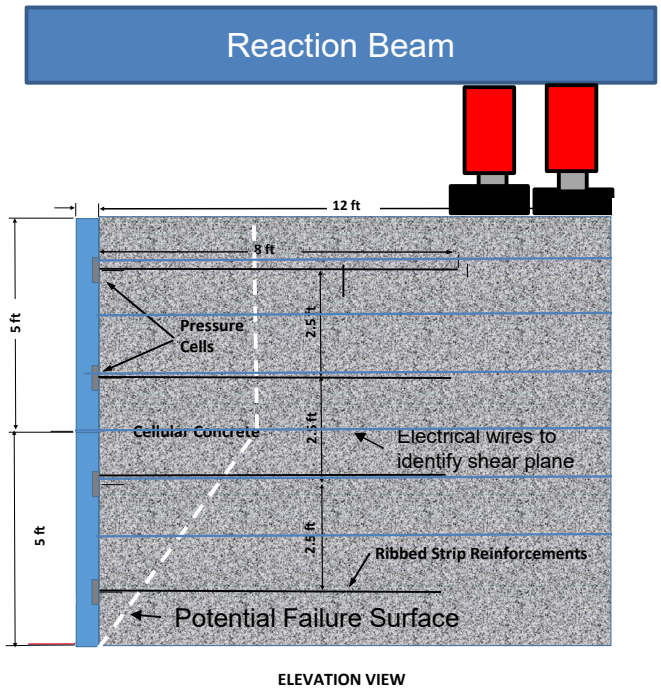

Fig. 3. Schematic drawings illustrating the surcharge load application for (a) the MSE wall test and (b) the free face wall test.

Test Results

A plot of the applied surcharge pressure versus axial displacement is provided in Fig. 4. The stiffness of the curve near the MSE wall is somewhat lower than that for the free face, but the difference is not large. However, at a surcharge pressure of about 44 psi, the axial settlement near the wall increases rapidly and the surcharge pressure decreases as the LCC loses strength after reaching its peak strength. In contrast, the test near the MSE wall continues to carry higher surcharge pressures up to a value of about 67 psi, where settlement increases to over 3 inches with a small decrease in surcharge pressure. Failure of the MSE wall exhibits relatively ductile behavior, while the free face does not.

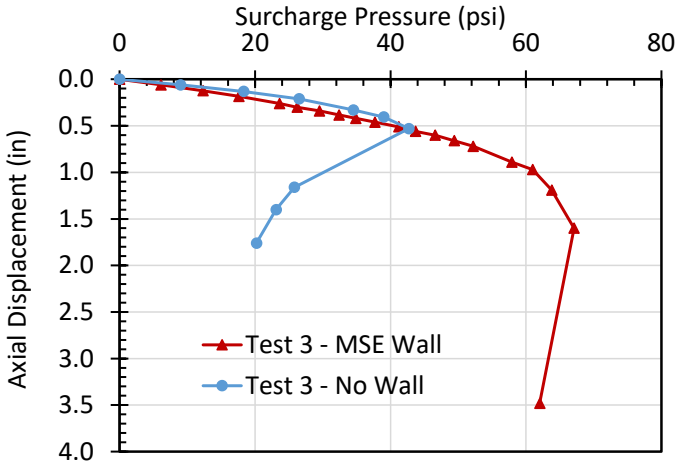

Fig. 4. Applied surcharge pressure versus axial displacement in the LCC for tests with and without MSE wall.

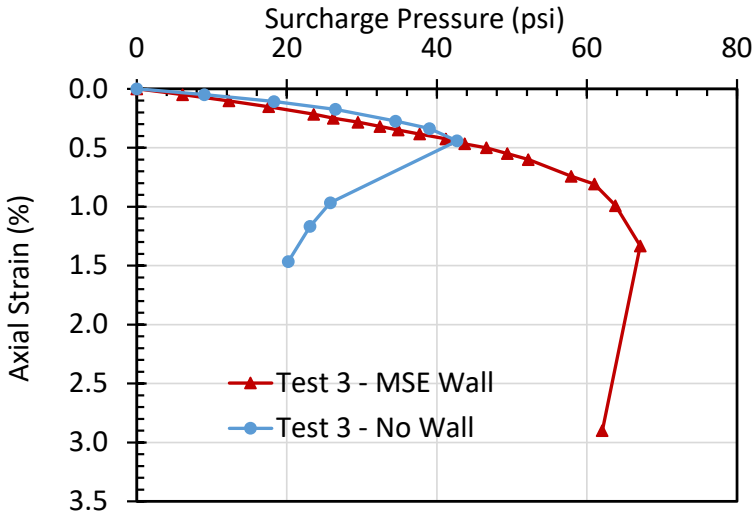

Fig. 5 Applied surcharge pressure versus axial strain in the LCC for tests with and without MSE wall.

Fig. 5 shows plots of surcharge pressure vs. axial strain for both wall tests. The curves show that failure occurred at axial strains of 0.5% and 1.35% for the free face and MSE wall tests, respectively.

A plot of applied surcharge pressure vs. lateral wall displacement is provided in Fig. 6 for both walls. The pressure vs. displacement curves are very similar until a pressure of 44 psi suggesting that the strength of the LCC provided most of the resistance to this point. At higher pressures, the curve for the free face experiences significant lateral displacement as surcharge pressure decreases. In contrast, the pressure vs. lateral displacement curve near the MSE wall continues to show an increase in resistance that must come primarily from the strength of the wall system. There is a significant reduction in stiffness at a surcharge pressure of about 60 psi and failure of the retaining wall occurs at a surcharge pressure of about 67 psi when the wall begins to deform without an increase in applied pressure.

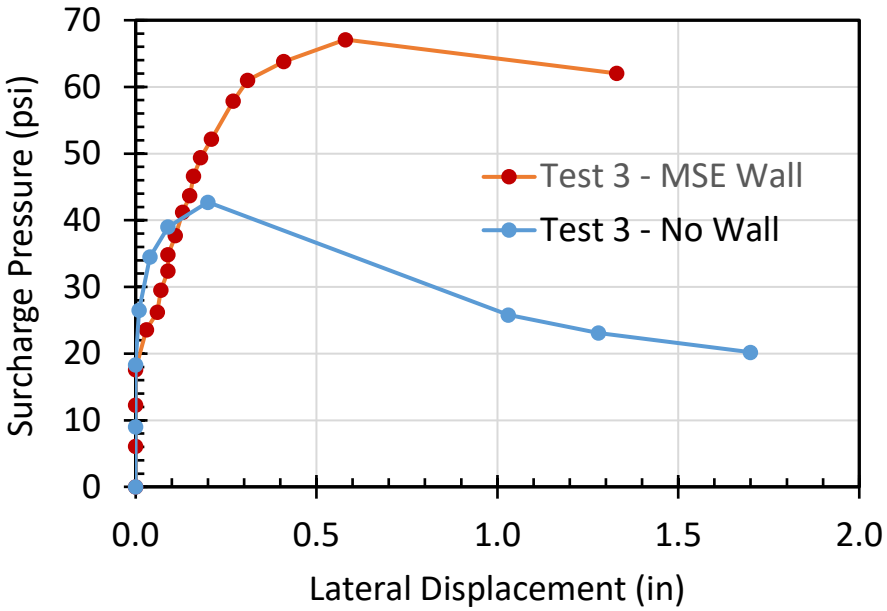

Fig. 6. Applied surcharge pressure vs. lateral wall displacement in the LCC for tests with and without RC cantilever retaining wall for unreinforced LLC test 2.

Fig. 7 provides a comparison of the surcharge pressure vs. lateral wall displacement for the first and second unreinforced LCC tests with the RC cantilever retaining wall. The unconfined compressive strength for both tests was approximately 100 psi. In addition, the surcharge area adjacent to the walls, 6 feet, was the same in both tests. The initial pressure vs. displacement curves are remarkably similar for both tests. Wall deflection begins to develop at a surcharge pressure of about 16 psi and the stiffness for both tests is linear up to a surcharge pressure of about 50 psi. At this point, the RCC wall begins displacing more rapidly and reaches a peak strength of 63 psi where failure occurs (displacement increases with no increase in strength). In contrast, the MSE wall develops additional resistance up to a peak of 67 peak and then experiences some post-peak decrease in strength as wall

displacement accelerates. The failure pressures in both cases are considerably lower than the unconfined compressive strength.

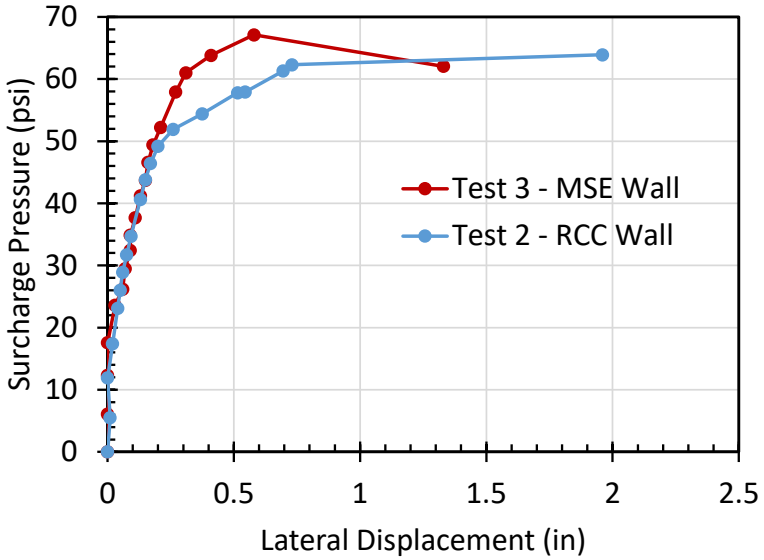

Fig. 7. Applied surcharge pressure vs. lateral wall displacement with MSE retaining wall for unreinforced LCC tests 1 and 2.

Fig. 8 provides a comparison of the surcharge pressure vs. lateral wall displacement for the unreinforced LCC tests and the first MSE wall tests adjacent to the free face (no retaining wall). For the unreinforced LCC test the surcharge pressure was applied over an area 6 feet back from the wall face, while the surcharge pressure was only applied over an area of 4 feet for the MSE wall test. Despite the smaller surcharge area, the failure surface initiated at a distance of 2 feet behind the wall in both cases. The pressure vs. lateral displacement curves for the two tests are nearly identical, in terms of initial stiffness, failure pressure, and post-peak strength reduction.

Fig. 9 provides plots of horizontal pressure on the RC wall vs. depth for selected applied surcharge pressures during loading as measured by the Geokon pressure plates. The other pressure sensors failed due to water infiltration. As the surcharge pressure increases, the pressures on the wall increase, but then appears to stabilize, for the most part, throughout the remainder of the test. We speculate that the initial horizontal pressure produced enough wall deflection to mobilize the resistance of the reinforcements which then picked up the additional load on the MSE wall panels.

Recent investigations by Tiwari et al. (2018) and Black (2018) have concluded that the shear strength of LCC can be approximated using a friction angle (ϕ) of 34° and a cohesion ranging from 700 to 1000 (Black 2018) or 700 to 1600 psf (Tiwari et al. 2018). If this strength model is adopted, then the horizontal pressure (σ_h) versus depth on the wall due to the LCC during surcharge loading can be computed using the equation

$$\sigma_h = \gamma z K_a + q K_a - 2c K_a^{0.5} \quad (1)$$

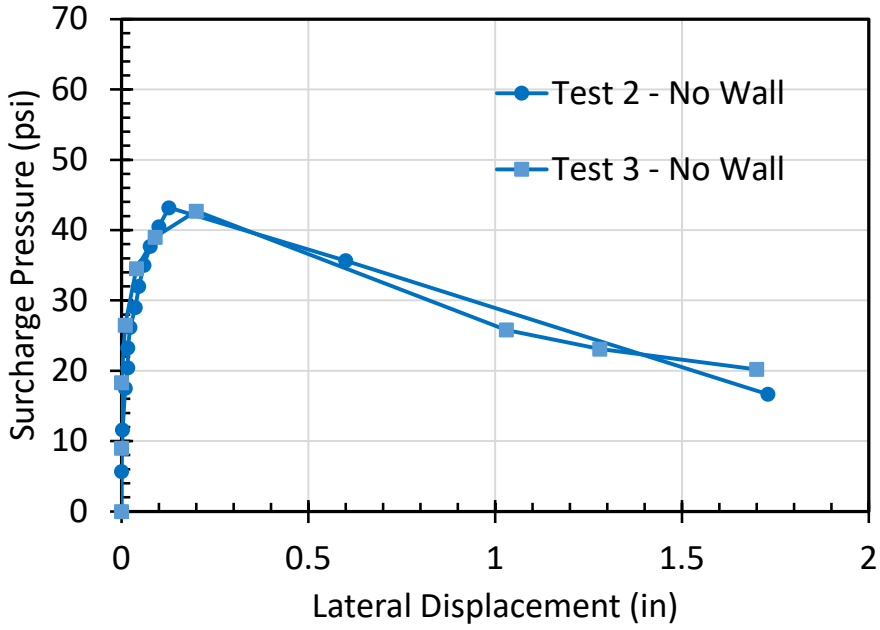

Fig. 8. Applied surcharge pressure vs. lateral wall displacement with no retaining wall (free face) for unreinforced LCC tests 1 and 2.

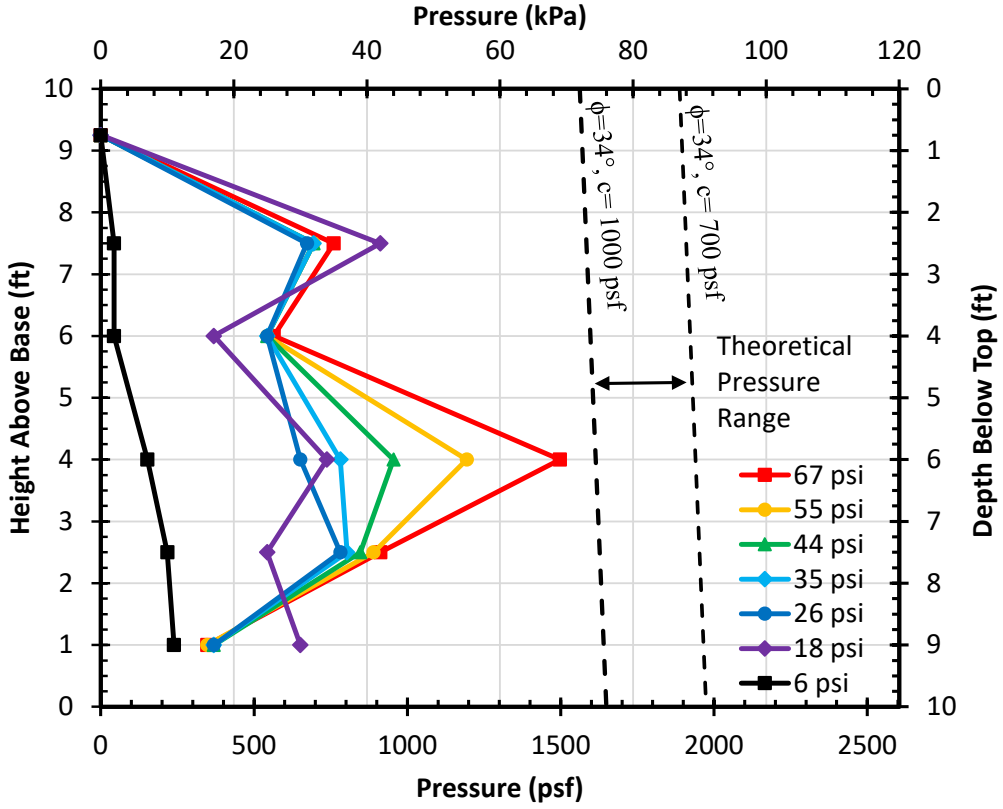

Fig. 9. Horizontal pressure on the RC wall versus depth curves for selected applied surcharge pressure values near the wall during test 2 as measured by Geokon pressure plates.

where $K_a=\tan^2(45-\phi/2)$, $\phi=34^o$, c=700 to 1000 psf, $\gamma=27$ lbs/ft^3, q=surcharge pressure, and z=depth below the ground surface. The range of theoretical horizontal pressures (c = 700 to 1000 psf) on the cantilever wall computed using Equation 1 is plotted relative to the measured horizontals pressure in Fig. 9. In the LCC test with the RCC wall, the pressures on the retaining wall approached the limits of the theoretical pressure curves. However, for the MSE wall test, the pressures on the MSE wall panels were only about half of the pressure on the RCC wall. Because lateral resistance for an MSE wall is largely designed to be produced by the reinforcements, not the wall, this result is consistent with expectations for the system.

Based on the string potentiometer measurements on the front face of the cantilever retaining wall, horizontal wall deflection has been plotted as a function of height above the base of the wall for selected surcharge pressures in Fig. 10. The string pots were located at the height of the MSE reinforcement connections. All displacement were less than about 0.25 inch for surcharge pressures up to 55 psi. At the peak surcharge pressure of 67 psi, wall deflection exceeded 0.50 inch with the maximum value at the top of the wall with deflection of about 0.1 inch at the bottom. As the strength decreased post-peak, the displacement of the MSE wall panels accelerated with the maximum value ultimately occurring at the joint between the two wall panels (5 ft). Overall, displacements of the top panel were greater than those on the bottom panel.

(a)

(b)

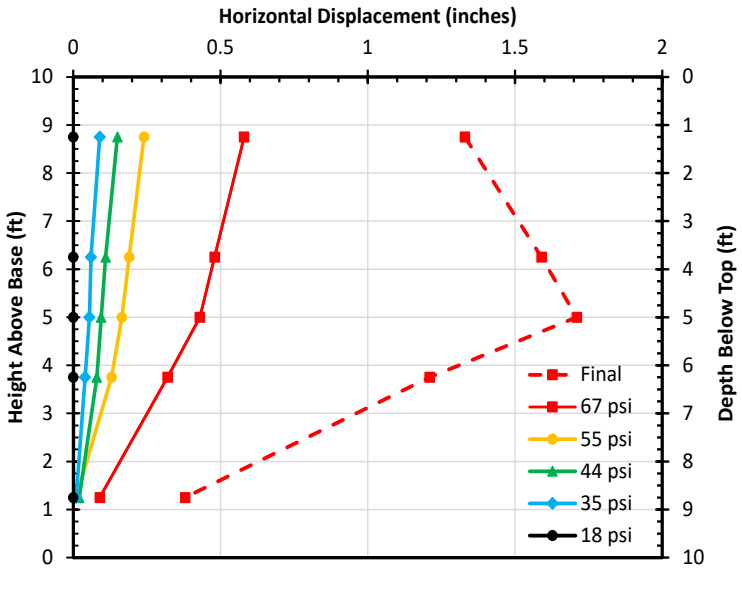

Fig. 10 (a) photograph of MSE wall panel deflection at failure, and (b) measured horizontal deflection of the wall versus height above the base of the wall for selected surcharge pressures.

At the completion of the test, one side wall and the back wall (free face) were both removed to provide a view of the crack patterns produced by the load testing. Drones were also used to photograph the LCC block from multiple angles to produce a 3D point cloud model of the deformed geometry using structure from motion software. Fig. 11 provides a photograph

from the side of the LLC block while Fig. 12 provides 3D point cloud representations of the crack patterns in the LCC block. The cracks painted in yellow likely developed during loading near the MSE wall, while the cracks painted in red likely developed during loading near the free face with no wall. The red cracks indicate that a nearly vertical shear plane developed at the back side of the third surcharge block (6 feet behind the wall), due to the 3 inch offset at the top of the LCC block (see Fig. 12 (b)), and propagated to a depth of about 5 feet (mid-height). The failure plane then appears to move to the base of the stem wall at an angle of 39° as shown in Fig. 11.

Fig. 11. Photo showing the yellow crack patterns adjacent to the MSE wall with the six-foot wide surcharge load at the surface. Red crack patterns are for a second test with four-foot wide surcharge adjacent to free-face without MSE wall. Reinforcement locations are shown by horizontal black lines.

This failure surface is similar to what would be expected for an MSE wall where the failure wedge extends vertically downward at a distance of 0.3H (3 feet) behind the wall to a depth of 0.5H (5 feet) and then slopes at an angle $45+\phi/2$. However, the vertical plane develops further back from the wall and the sloped section is flatter, in this case. The series of vertical yellow cracks in the lower half of the wall suggests that a “toppling” type of failure may initially combine with a subsequent shear failure plane to apply pressure to the MSE wall.

In the absence of a retaining wall, the pattern of shear planes and cracks develops much closer to the wall face than was observed near the cantilever wall. Although a relatively uniform surcharge pressure was applied to a distance of four feet from the wall, a shear plane developed in the LCC just behind the first surcharge block at a distance of two feet behind the

wall. A significant vertical offset is observed across the top of the LCC block in Fig. 12 (a). The shear crack propagates nearly vertically to a depth of about 5 ft (mid-height of the wall), then slopes down to the base of the wall at an angle of 62° from the horizontal as shown in Fig. 11. This failure angle is obviously much steeper than was observed in the LCC behind the cantilever wall.

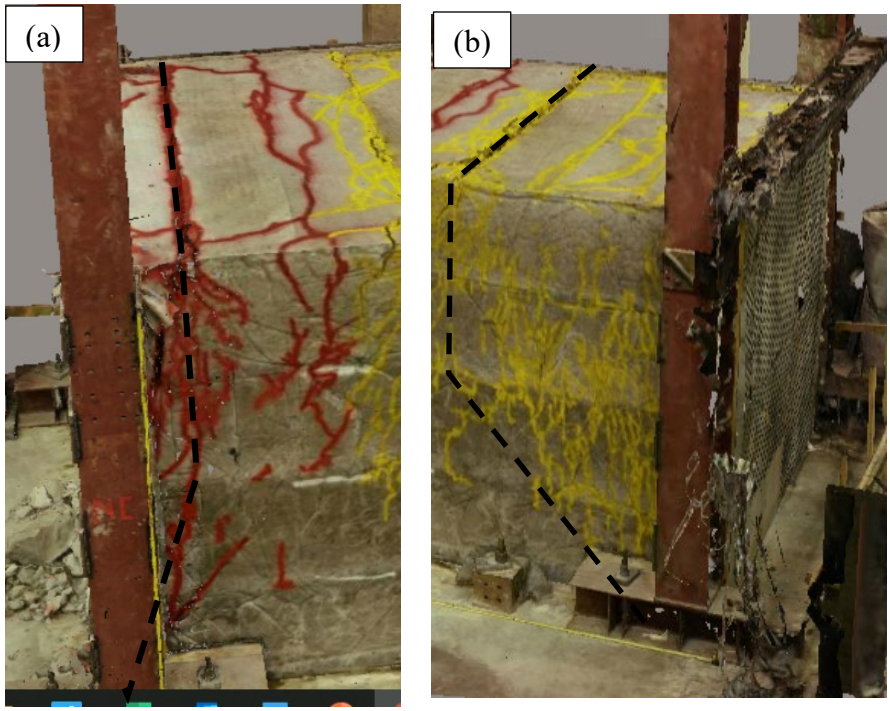

Fig. 12. Three-dimensional point cloud models of (a) crack patterns due to surcharge loading near the free face without a wall and (b) crack patterns due to surcharge loading near the RC retaining wall. (URL for interactive 3D point cloud models). http://prismweb11.groups.et.byu.net/Block3RollinsEdits/App/?#%2F

If the angle of inclination of the failure slope is assumed to be equal to $45 + \phi/2$, as would be the case of an active earth pressure failure, then the back-calculated friction angle is 34°, which is the friction angle that has been recommended for LCC, as discussed previously (Tiwari et al. 2018, Black 2018).

When the wood panel was removed on the back face of the box after completion of the load test on the MSE wall side of the box, no vertical cracks were observed in the free face. This result suggest that the wall was relatively unaffected by the loading on the other side of the box. During the first set of unreinforced LLC tests, when a surcharge was placed over the entire LCC surface, many vertical cracks were observed in the free face. A photograph of the free face at the completion of the surcharge loading adjacent to the free face is shown in Fig. 13. The cracks were spray-painted with red paint to highlight their locations. The cracks consist of both vertical and horizontal or inclined cracks. Visual observations at the time that the wall was failing indicated that the top half of the wall appeared to be moving as an intact

block that was sliding downward on top of the underlying shear planes. Surcharge loading was halted to prevent the sliding mass from reaching complete failure.

Fig. 13. Photograph of the crack pattern in the LCC on the free face opposite to the MSE retaining wall side.

Preliminary Conclusions

1. LCC walls can successfully withstand significant surcharge loadings with limited axial and lateral deformations. However, failure or excessive displacement occurs at surcharge pressure much less than the unconfined compressive strength (UCS).

2. The presence of an MSE wall significantly increased the strength of the LCC block and led to a more ductile rather than a brittle failure with a significant loss of strength.

This result strongly indicate the improved performance produced by the MSE wall reinforcement.

3. Measured horizontal pressures at the back of the MSE wall panels were only about half of what would be expected using Rankine earth pressure theory using a friction angle (ϕ) of 34° and a cohesion of 700 to 1000 psf. This result is expected because the MSE reinforcements are expected to carry the lateral pressure rather than the wall panels.

4. Failure surfaces for the free face wall with unreinforced LCC were much steeper and shallower than those supported by the MSE wall. The steeper failure surface in the lower half of the wall was generally consistent with a Rankine active earth pressure with a friction angle of 34°.

5. The failure surface for the LCC behind the RC cantilever retaining wall shows a bi-linear shape typical of soil backfill with MSE wall reinforcements that provide an effective cohesion. The composite failure surface is vertical to about 50% of the wall height and then inclines towards the connection between the base of the wall.